HHS Public Access

Author manuscript

Mult Scler. Author manuscript; available in PMC 2020 August 13.

Published in final edited form as:

Mult Scler. ; : 1352458519828667. doi:10.1177/1352458519828667.

Higher EBV response is associated with more severe gray matter and lesion pathology in relapsing multiple sclerosis patients: a case-controlled magnetization transfer ratio study

Dejan Jakimovski[1], **Murali Ramanathan**[2], **Bianca Weinstock-Guttman**[3], **Niels Bergsland**[1], **Deepa P. Ramasamay**[1], **Ellen Carl**[1], **Michael G. Dwyer**[1], **Robert Zivadinov**[1,4]

[1]Buffalo Neuroimaging Analysis Center, Department of Neurology, Jacobs School of Medicine and Biomedical Sciences, University at Buffalo, State University of New York, Buffalo, NY, USA;

[2]Department of Pharmaceutical Sciences, Jacobs School of Medicine and Biomedical Sciences, University at Buffalo, State University of New York, Buffalo, New York, USA;

[3]Jacobs MS Center, Department of Neurology, Jacobs School of Medicine and Biomedical Sciences, University at Buffalo, State University of New York, NY, USA

[4]Center for Biomedical Imaging at Clinical Translational Science Institute, University at Buffalo, State University of New York, Buffalo, NY, USA;

Abstract

Background.—Epstein Barr virus (EBV) infection has been associated with higher clinical activity and risk of multiple sclerosis (MS).

Objective.—To evaluate associations between EBV-specific humoral response and magnetization transfer ratio (MTR)-derived measure in MS patients and healthy controls (HCs).

Methods.—The study included 101 MS patients (69 relapsing-remitting MS (RRMS) and 32 secondary-progressive MS (SPMS)) and 41 HCs who underwent clinical, serological, and MRI investigations. MTR values of T1-, T2-lesion volume (LV), normal-appearing (NA) brain tissue (NABT), gray matter (NAGM) and white matter (NAWM) were obtained. Enzyme-linked immunosorbent assay was used to quantify EBV antibody levels. Partial correlations corrected for

Corresponding Author: Robert Zivadinov, MD, PhD, FAAN, FEAN, FANA, Center for Biomedical Imaging at Clinical Translational Science Institute, Buffalo Neuroimaging Analysis Center, Department of Neurology, Jacobs School of Medicine and Biomedical Sciences, University at Buffalo, State University of New York, 100 High Street, Buffalo, NY 142013, Phone: 716-859-7040, Fax: 716-859-7066, rzivadinov@bnac.net.

Disclosures

Financial Relationships/Potential Conflicts of Interest:

Dejan jakimovski, Niels Bergsland, Deepa P. Ramasamy and Ellen Carl have nothing to disclose. Murali Ramanthan received research funding the National Multiple Sclerosis Society, the National Institutes of Health and Otsuka Pharmaceutical and Development. These are unrelated to the research presented in this report.

Michael G. Dwyer has received consultant fees from Claret Medical and research grant support from Novartis.

Bianca Weinstock-Guttman received honoraria as a speaker and as a consultant for Biogen Idec, Teva Pharmaceuticals, EMD Serono, Genzyme& Sanofi, Novartis and Acorda. Dr Weinstock-Guttman received research funds from Biogen Idec, Teva Pharmaceuticals, EMD Serono, Genzyme& Sanofi, Novartis, Acorda.

Robert Zivadinov received personal compensation from EMD Serono, Genzyme-Sanofi, Claret Medical, Celgene and Novartis for speaking and consultant fees. He received financial support for research activities from Genzyme-Sanofi, Novartis, Claret Medical, Intekrin-Coherus and IMS Health.

MRI strength were used and Benjamini-Hochberg-adjusted p-values <0.05 were considered significant.

Results.—MS patients had significantly higher anti-EBNA-1 titer when compared to HCs (107.9 U/ml vs. 27.8 U/ml, p<0.001). Within the MS group, higher serum anti-EBNA-1 titer was significantly correlated with lower T1-LV MTR (r=−0.287, p=0.035). Within the RRMS group, higher serum anti-EBNA-1 titer was associated with T1-LV MTR (r=−0.524, p=0.001) and NAGM MTR (r=−0.308, p=0.043). These associations were not present in HCs or SPMS patients.

Conclusion.—Greater EBV humoral response is associated with lower GM MTR changes and focal destructive lesion pathology in RRMS patients.

Keywords

MTR; EBV; EBNA-1; demyelination

Introduction

Multiple sclerosis (MS) is a chronic autoimmune disease of the central nervous system (CNS) characterized by early episodic demyelinating attacks and continuous neurodegenerative changes of the white and gray matter (WM and GM).[1] Although an interplay of multiple genetic, environmental, and cardiovascular risk factors have been suspected, the exact and specific MS pathophysiology still remains to be elucidated. Among the many proposed environmental contributors to MS pathogenesis, late primary Epstein-Barr virus (EBV) infection has remained as an important and continuously documented risk factor.[2] The exposure and extent of the EBV infection can be measured with a panel of anti-EBV biomarkers, including antibodies towards the anti-EBV early antigen (EA), anti-EBV viral capsid antigen (VCA), and anti-EBV nuclear antigen (EBNA).[2] In comparison to the anti-VCA antibodies which appear and peak during the early phase of the infectious course, the anti-EBNA-1 antibodies emerge slowly after 2–4 months of the symptom onset and may be correlated to the load of latent EBV-infected B-cells.[2]

Accumulating evidence on the increasingly important role of B-cells in MS pathophysiology has been recently reported.[3] Moreover, the role of B-cells has been additionally corroborated by the recent success of B-cell depleting therapies in decreasing MS-related disease activity.[4] The memory $CD27^+$ B-cells have been especially related to the extent of the MS pathology and they present with specific receptors that are used by the EBV to bind, infect, and consequently immortalize the cells.[5] Therefore, they provide suitable environment for survival of undetectable and relatively stable levels of latent virus in which infected B-cells act as the EBV reservoir. Furthermore, recent molecular studies demonstrated that EBV-induced B-cells increase in myelin immunogenicity and autophagy.[6] EBV infection allows upregulation of antigen-presenting capability of the B-cells by activating and streamlining the internal processes into more effective myelin presentation.[6] Therefore, the pool of EBV-infected B-cells would provide higher T-cell activation, ultimately leading to a larger attack towards brain myelin.

The effect of EBV infection on MRI-detected MS pathology has been only investigated with conventional measures like contrast-enhancing lesions, T2 or T1 lesion volume and global brain volumes.[2] Studies examining both clinically definite MS and clinically isolated syndrome (CIS) patients have demonstrated associations between higher humoral response towards EBV with both greater T1 and T2 lesion number, lower cross-sectional brain volumes, and increased longitudinal atrophy rates.[7, 8] Furthermore, relapsing-remitting MS (RRMS) patients with the highest titer of anti-EBV antibodies showed more advanced neurodegenerative pathology, as indicated by increased T1 lesion number and greater cortical atrophy.[7] However, conventional MRI measures may not fully capture the full extent EBV's effect on myelin damage.

Magnetization transfer imaging (MTI) is a nonconventional MRI technique that has been increasingly utilized in MS studies.[9] The MTI-derived magnetization transfer ratio (MTR) relates to myelin status, axonal loss, and cell infiltration changes.[10] For an example, lower MTR values have been previously corroborated with histopathological loss of WM and GM myelin content.[10, 11] Therefore, the MTI technique is a convenient, non-invasive method to investigate associations between hypothesized contributors to potential MS-related demyelination or remyelination processes.[12]

Based on this background, we hypothesized that MS patients with higher humoral anti-EBV response will present with lower brain myelin levels as measured by *in vivo* MTI.

Materials and Methods

Study population:

The study population utilized in this analysis was part of a larger, prospective study of cardiovascular, environmental and genetic (CEG) risk factors in MS that enrolled over 1,000 subjects with clinically isolated syndrome, MS, healthy controls (HCs) and other neurologic diseases (OND). This sub-study inclusion criteria were: 1) Age of 18–75 years old, 2) being a MS patient as diagnosed by the 2010-revised McDonald criteria,[13] 3) being a healthy control (HC) without prior or current neurological disorder, 4) obtaining MRI with standardized protocol that included specific MTI sequence on 1.5T or 3T scanners, 5) clinical examination within 30 days from the MRI visit and 6) serum samples obtained at the day of the MRI examination for EBV status determination. On the other hand, the exclusion criteria included: 1) clinical relapse or steroid use within 30 days of the MRI visit and 2) pregnant or nursing mothers. An experienced neurologist performed full clinical and neurological examination and the Kurtzke's Expanded Disability Status Scale (EDSS) scores were determined.[14] With use of standardized study questionnaires, additional information regarding the history of mononucleosis was collected.

The study participants signed written informed consent and the study was approved by the University at Buffalo Institutional Review Board (IRB).

MRI acquisition and analysis:

The MS patients were scanned using either 3T or 1.5T General Electric Signa Excite HD 12.0 Twin Speed 8-channel scanners (GE, Milwaukee, WI, USA) and 8 channel head and

neck (HDNV) receive coil using standardized MRI protocols, whereas the HC were scanned only on the 3T scanner with the same protocols. Of the 101 MS patients, 62 were scanned on 3T scanner and 39 were scanned on the 1.5T. The 3T sequences used included: 1) 2D Fluid Attenuated Inversion Recovery (FLAIR) with TE/TI/TR of 120msec/2100msec/8500msec, field of view (FOV) of 25.6cm × 19.2cm, flip angle of 90°, slice thickness of 2mm with no gap, and total acquisition time of 5 minutes and 16 seconds; 2) 3D T1-weighted imaging (WI) fast, spoiled, gradient echo with magnetization prepared inversion recovery pulse (IR-FSPGR) with TE/TI/TR of 6.6msec/2.8msec/900msec, FOV of 25.6cm × 19.2cm, flip angle of 10°, slice thickness of 1mm with no gap, and total acquisition time of 9 minutes and 18 seconds; and 3) 3D gradient recalled echo (GRE) with TE/TR of 6msec/50msec, flip angle of 10°, bandwidth of 122.10kHz, slice thickness of 4mm with no gap, phase FOV of 75, with and without additional magnetization transfer frequency saturation offset pulse of 1500 Hz, and acquisition time of 6 minutes and 52 seconds. On the other hand, the 1.5T utilized 1) 2D FLAIR TE/TI/TR of 126msec/2000msec/8000msec, FOV of 25.6cm × 19.2cm, flip angle of 90°, slice thickness of 3mm and total acquisition time of 3 minutes and 12 seconds; 2) 3D T1-WI IR-FSPGR with TE/TI/TR of 3.7msec/900msec/5.9msec and FOV 25.6cm × 19.2cm, flip angle of 10°, slice thickness of 1.5mm with no gap, and acquisition time of 8 minutes and 50 seconds; 3) 1.5T 3D GRE with TE/TR of 6msec/50msec, flip angle of 10°, bandwidth of 122.10kHz, slice thickness of 5mm with no gap, phase FOV of 100 with and without additional magnetization transfer frequency saturation offset pulse of 1500 Hz with acquisition time of 5 minutes. Detailed description of MRI acquisition parameters are provided in the MRI appendix material.

A semi-automated contouring/thresholding technique was used to measure the T1 and T2 lesion volume (LV) masks, as described elsewhere.[15] Additionally, the global tissue segmentations of gray matter (GM) and white matter (WM) were obtained by SIENAX cross-sectional software (version 2.6, FMRIB, Oxford, UK).[16] T1 hypointensities were filled prior to segmentation to avoid tissue misclassification.[17] Normal-appearing brain tissue (NABT), normal-appearing white matter (NAWM), and normal-appearing (NAGM) were derived after removing voxels that corresponded to the T2 lesions.

As previously published, the MTR values were calculated by digital subtraction and use of the standardized formula of:

$$MTR = \left(\frac{M_0 - M_s}{M_0}\right) \times 100 \text{ where,}$$

M_0 is the pixel intensity of the sequence without the MT pulse and M_s is the same pixel with the MT pulse. Mean MTR values were calculated within lesions, NABT, NAWM, and NAGM. All analysis was performed blinded to clinical characteristics.

EBV humoral response analysis:

The status of anti-EBNA-1 IgG antibodies was determined by the Department of Pharmaceutical Sciences at University at Buffalo. Analysis was blinded to the clinical status and the severity of the MS disease. Enzyme-linked immunosorbent assay (ELISA) kit

(Diamedix Corporation, Miami, FL, USA) was used to quantify the antibody levels, which were normalized based on the manufacturer's cut-off standards. Serial dilution of manufacturer-provided positive control samples allowed generation of standard curves.[7] The cut-off was calibrated by manufacturer-provided plasma which is weakly reactive to anti-EBNA-1 antibodies. The quality control was additionally performed by paired sera controls (Index Value between 3.0 and 4.0), which underwent 4-fold dilution. Both the low positive (low range of the assay) and negative control were included in each test run. The study subject sera was diluted in 1:21 ratio.

Statistical analysis:

The statistical analysis were performed using SPSS 25.0 (IBM, Armonk, NY, USA). For demographic and clinical comparisons between the HCs and MS patients, χ^2 test, Student's t-test and Mann Whitney U-test were used according to the normality of the data. The normal distribution of the data was determined using Kolmogorov-Smirnov. The data distribution was further analyzed with Q-Q plot visualization. Due to the non-parametric nature of the anti-EBNA-1 titer and the MTR values, the Spearman's non-parametric rank correlations were utilized. Furthermore, quartile analysis based on the anti-EBNA-1 titer was performed. Since 39 MS patients were acquired on 1.5 T scanner and 62 on 3T scanner, partial non-parametric correlation corrected for the MRI field strength was utilized. Lastly, the partial non-parametric correlations were repeated, correcting for disease duration.

In order to graphically illustrate the data, scatter plots were employed, where both the MTR values and anti-EBNA-1 titer were transformed using the natural logarithm. Both for the MS vs. HCs and the RRMS vs. SPMS analyses, multiple comparison correction/false discovery rate (FDR) was performed using the Benjamini-Hochberg procedure and adjusted p-values lower than 0.05 were considered statistically significant. Post-hoc power analysis for the significant findings determined the minimal sample size based on study power at 60%, 70%, 80%, 90% and 95%. (Supplement Table 1). Lastly, the differential relationship of anti-EBNA-1 titer and the MTR values seen between different MS phenotypes was tested by general linear model (GLM) analysis. The associations between brain MTR values and the interaction between disease phenotype and anit-EBNA-1 levels was additionally reported.

Results

Study population:

The demographic, clinical, and MTR characteristics of the study population are shown in Table 1. The study population consisted of 41 HCs and 101 MS patients who showed no significant differences in age (mean 45.4 vs. 46.9, *t*-test p=0.681) and sex (29/12 vs. 75/26 female to male ratio, χ^2 p=0.679). Although numerically higher, the history of mononucleosis was not different between the HC and MS patients (17.1% vs. 33.7%, χ^2 p=0.126). The disease-modifying treatments (DMTs) used by the MS patients included interferon-β (36.6%), glatiramer acetate (24.8%), natalizumab (19.8%), off-label medications (3.9%) and 15 patients (14.9%) were not on any DMT.

Similarly, Table 2 demonstrates the demographic, clinical, and MTR characteristics of the RRMS and secondary-progressive (SP) MS subgroups. The SPMS group was older (mean 52.3 vs. 44.4, *t*-test p=0.001), had longer disease duration (mean 19.9 vs. 10.2, *t*-test p=0.002) and was more disabled (median EDSS of 6.0 vs. 2.0, Mann-Whitney U-test p<0.001). There were no differences in the sex ratio between the SPMS and RRMS groups (51/18 vs. 24/8 female to male ratio, χ^2 p=1.000) nor in use of DMTs (χ^2, p=0.337).

As expected, the MS patients had lower MTR values compared to HC in the NABT (median 40.0 vs. 42.0, Mann Whitney U-test p<0.001), NAWM (median 44.0 vs. 46.0, Mann Whitney U-test p<0.001), NAGM (median 37.0 vs. 39.0, Mann Whitney U-test p<0.001) and MTR of T2 lesions (median 41.0 vs. 45.0, Mann Whitney U-test p<0.001) (Table 1). On the contrary, there were no statistical difference in the MTR values between RRMS and SPMS patients (Table 2). The comparison between the groups using only 3T-derived MTR values yielded similar statistical differences.

Differences in anti-EBNA-1 titers between healthy controls and multiple sclerosis patients:

The serum-derived anti-EBNA-1 titer of the HCs, MS patients, and their respective RRMS and SPMS subgroups are shown in Table 1 and 2. The MS patients had higher anti-EBNA-1 titer when compared to the HC population (median 107.9 U/ml vs. 27.8 U/ml, Mann-Whitney U-test p<0.001). Although numerically higher in the RRMS group, there were no significant anti-EBNA-1 titer differences between the RRMS and SPMS subgroups (median 132.6 U/ml vs. 80.4 U/ml, Mann-Whitney U-test p=0.635).

Magnetization transfer ratio associations with serum anti-EBNA-1 titer levels in healthy controls and multiple sclerosis patients:

Within the MS patients, higher serum anti-EBNA-1 titer was significantly associated with lower T1 lesion MTR (r=−0.287, p=0.035). The serum anti-EBNA-1 titer was not associated with the MTR measures value in HC. (Table 3). The MS population was also categorized based on anti-EBNA-1 titer quartiles (Supplement Figure 1) and both T1 lesion MTR and NAGM MTR values were the lowest within the first quartile (one-way ANOVA, p=0.001 and p=0.023, respectively). There were no age nor disease duration differences between the anti-EBNA-1 quartiles.

Likewise, the RRMS patients showed associations of higher serum anti-EBNA-1 titer and lower T1 lesion MTR (r=−0.524, p<0.001) and NAGM (r=−0.308, p=0.043) (Table 4). In contrast, these associations were not present within the SPMS group. Additional analysis utilizing dichotomization based on the median NAGM MTR values was performed. RRMS patients within the lower NAGM MTR group had significantly higher anti-EBNA-1 titer when compared to the RRMS group with the higher NAGM MTR (median 195.8 vs. 53.4, p<0.001) The graphical representation of the findings is shown in Figure 2. The effect of the disease phenotype on the association between the T1 lesion MTR values and anti-EBNA-1 titer was confirmed by the GLM analysis (interaction effect of $F_{1,97}$=9.05, p=0.004). On the other hand, such interaction between the disease phenotype and anti-EBNA-1 titer was not significantly associated with the NAGM MTR values ($F_{1,97}$=2.25, p=0.137).

Separate analysis within the smaller MS population scanned only on the 3T scanner (Supplement Table 2) confirmed the association between higher anti-EBNA-1 titer and lower T1 lesion MTR values (r=−0.353, p=0.022 and r=−0.532, p=0.007, for total MS population and RRMS only, respectively). The association between higher anti-EBNA-1 titer and T1 lesion MTR is additionally illustrated in Figure 1 and a case example of an RRMS patient with potentially large pool of EBV-infected B-cells (measured as very high anti-EBNA-1 titer), and accompanying T1-hypointensities is demonstrated in Figure 3. After correcting for the disease duration, the correlations between anti-EBNA-1 titer and T1 lesion MTR in the total MS population (r=−0.265, FDR-unadjusted p=0.023), anti-EBNA-1 titer and T1 lesion in RRMS (r=−0.503, FDR-unadjusted p<0.001), and anti-EBNA-1 titer and NAGM in RRMS (r=−0.3, FDR-unadjusted p=0.014) remained significant.

Discussion

This is one of the first studies to demonstrate an association between greater anti-EBV humoral response and *in-vivo*, MRI-derived, lower global and MS lesion MTR levels. Conversely, these associations were not observed in the age-matched HC population. The associations of higher anti-EBNA-1 levels and potentially lower myelin levels were primarily driven by the active RRMS cohort and located at sites of T1 lesions, and in the NAGM.

Late EBV infection has been implicated as a contributor to increased risk of developing MS and further increased disease activity.[18] Several studies have shown an association of higher serum anti-EBNA-1 IgG antibodies and a “dose-dependent” increase of the MS risk.[19] Individuals with IgG titers higher than 320U/ml had 36-fold higher MS risk when compared to individuals with <20U/ml, and 8-fold higher when compared to individuals with <320U/ml.[19] In line with previous reports, the MS patients from our cohort had 4-fold higher anti-EBNA-1 levels when compared to the HCs. Furthermore, MS patients had double the frequency of infectious mononucleosis, a difference that was not significant, probably because of the relatively low sample size of the study. Several epidemiological studies have demonstrated associations between history of infectious mononucleosis and consequently increased risk of MS.[20, 21] Since the development of MS cannot be attributed to any single factor, the interplay of environmental effects should be assessed as a joint effect of their interactions.[22] A recent study calculated the attributable fraction for each known MS risk factor and concluded that previous history of infectious mononucleosis constitutes 30.8% of the total environmental effect.[22]

Previous studies have only examined the association between active EBV infection and conventional MS-related MRI-detected pathology.[23, 24] For an example, MS patients with cerebrospinal fluid presence of EBV DNA do present with more gadolinium-enhancing lesions.[25] Similarly, a larger cross-sectional study showed that patients within the highest quartile of anti-VCA levels had significantly higher T2-LV, higher number and volume of T1-hypointensities and lower brain volume.[7] In line with our association of higher anti-EBV response and lower NAGM myelin levels, the previous study also showed an association of greater cortical pathology and higher anti-EBV levels, a finding which was only seen within the relapsing MS group.[7] To the best of our knowledge, this is the first report regarding the

effect of EBV and *in vivo* MTR-derived myelin content and thus provides further evidence regarding the supposed role of EBV in MS pathology.

Multiple latent and lytic EBV proteins, like the latent membrane protein 1 (LMP-1) and the immediate-early lytic gene product (BZLF1), have been detected in MS brains with prevalent presence of $CD138^+$ plasma cells. Furthermore, our finding of an association between high anti-EBNA-1 titer and lower T1 lesion MTR was further corroborated by reports of immunohistochemical demonstration of the lytic EBV phenotype within chronic MS lesions.[26] Similarly, a recent histopathological study utilized laser-cut SPMS lesioned brain samples and demonstrated upregulation and expression of diversity of genes associated with latent EBV infection such as EBNA3A, LMP1, and LMP2A.[27] Conforming to our example demonstrated in Figure 3, recent fulminant and lethal relapse of a natalizumab-discontinuing RRMS patient has been attributed to extensive demyelination and infiltration of EBV-infected B-cells.[28] Since most histopathological studies are performed on autopsied brains from patients with longstanding SPMS, they may not reflect the full scope of EBV's effect earlier in the disease. The significant associations found in this study were restricted to the RRMS group, findings in line with the early clinical effect of EBV on the increased MS risk and on increased relapse rate. Our general linear model additionally corroborated the differential phenotype effect, demonstrating specific RRMS contribution. Moreover, the findings between the higher anti-EBNA-1 titer and decreased MTR signal remained significant even after correction for patients' disease duration. Therefore the specific findings of lower MTR signal may be temporally restricted within the period of inflammatory activity which results with both pathological changes like acute demyelination and edema and concurrent B-cell influx and viral particle shedding.

On the other hand, lower NAGM MTR may potentially be explained by either presence of B-cell infiltrated intracortical lesions or by local cortical demyelination associated with meningeal, EBV-infected, B-cell-rich, tertiary lymphoid follicles. A postmortem examination of SPMS patients has demonstrated the presence of early EBV lytic proteins (BZLF1 and BFRF1) in all of the examined intracortical perivascular spaces.[29] Furthermore, the study also showed that cortical lesions themselves were infiltrated with EBV-infected B-cells, which may provide local maintenance of the B-cell driven inflammatory process.[29]

A subset of MS patients presents with intrameningeal follicles, which contain proliferating B-cells, strongly suggesting formation of an immune germinal center.[30] Therefore the follicle-like structures might represent a site of constantly maintained intracerebral pool of EBV-harboring B-cells.[31] In line with the proposed meningeal origin of cortical demyelination, quantitative assessment of cases with presence of the aforementioned follicles had 6-fold greater lesioned GM area and 3-fold greater total cortical demyelination.[32] On the other hand, patients with tertiary follicle-like structure had no statistical difference in the amount of lesioned WM area.[32] The ectopic B-cell-rich, follicle-like structures additionally contribute to a gradient of demyelination, greatest at the pial surface. This finding would implicate the diffusion of soluble factors that originate from the B-cells located in the meninges.[33] In addition to demyelination, there is also a gradient affecting both GM lesions, death of oligodendrocytes, increased microglial activation, and overall decrease in neuron density.[33] Furthermore, leptomeningeal perivascular inflammation can be

demonstrated *in vivo* by long-delay, post-contrast 3D FLAIR imaging and visualization of leptomeningeal contrast enhancement.[34] A post-mortem autopsy study also confirmed subpial confluent cortical demyelination around the sulci, which harbor the aforementioned abnormal contrast retention.[35] Although the presence of the meningeal tertiary follicle-like structures are usually associated with long-standing progressive MS disease, a recent report has demonstrated their presence in early and acute MS patients.[36] The overall cortical pathology seen in these early MS patients (2 years of disease duration) was highly associated with presence of meningeal inflammation.[36] More importantly, almost 20% of the GM lesions seen within the early MS patients with leptomeningeal inflammation were classified as actively demyelinating ($CD68^+$ macrophages which contain myelin inclusions). Conversely, despite the presence of meningeal follicles, none of the SPMS patients presented with actively demyelinating lesions.[36]

The discrepancies in the RRMS vs. SPMS associations may be further explained by the location of the EBV-infected B-cells and the availability to shed viral particles into the circulation. Although SPMS patients have higher percentage of leptomeningeal tertiary follicles, those EBV-infected B-cells may be fully compartmentalized behind an already repaired blood-brain barrier (BBB). On the other hand, EBV-infected B-cells that are actively participating within an acute lesioned process have the concurrent availability of disrupted BBB which would allow shedding of viral particles into the circulation. This working hypothesis can be supplemented by a recent attempt to deplete the meningeal B-cells by intrathecal administration of anti-CD20 agents. Initial mice model studies showed that administration of anti-CD20 medications are able to deplete the meningeal B-cells.[37] Based on these preclinical findings, early phase I clinical trials were initiated.[38] Progressive MS patients with MRI-documented leptomeningeal contrast enhancement (suggestive of meningeal B-cell accumulation) were treated with intrathecal anti-CD20 medication.[38] Although the treatment resulted with successfully depleted peripheral B-cells population, the medication did not change the initial extent of meningeal inflammation.[38] Therefore, the compartmentalized nature of the SPMS EBV-infected B-cells may prevent free diffusion of viral particles and ultimately diffusion of the targeted therapy.

One potential limitation of this study is the use of additional MS patients that were scanned on 1.5T MRI scanner. However, this further increased our sample size and the independent analyses demonstrated a similar effect in both groups regardless of the scanner used. Another potential limitation is the interpretation of the MTR changes. Although lower MTR levels have been histologically associated with lower myelin content, this measure may be additionally influenced by axonal damage and swelling. A recent investigation suggested that the T1-weighted hypointensities and the MTR signal can be considerably affected by axonal swelling, activation of the microglia, astrocytosis and serum proteins despite the absence of demyelination.[39] Analysis of the tertiary meningeal follicles, their harboring EBV load, and local GM demyelination may explain our findings. Future MTR and EBV studies in MS patients with and without presence of leptomeningeal contrast enhancement are needed. Future improvement in susceptibility-based imaging and classification of chronically-active (slowly-expanding) vs. inactive lesions may further help in pinpointing the factors that influence the anti-EBNA-1 and T1 lesion MTR association.[40] Given the controversial nature of the overall EBV effect on MS pathology, activity, and progression,

the findings should be carefully considered and further replicated. Potential analysis regarding the effect of B-cell depleting therapy on the EBV titer is also highly warranted. Finally, while our study was powered at 80% to show the association between anti-EBNA-1 and MTR of T1-LV and NAGM (Supplement Table 1) in total and RRMS population, the SPMS cohort was underpowered to investigate these associations. The finding of different EBNA-T1 MTR relationships between the RRMS and SPMS phenotypes should be further examined. Therefore, future studies including larger sample size of SPMS patients should explore these associations.

In conclusion, we demonstrated an association between greater humoral response towards EBV and more severe pathology within chronic T1-hypointense lesions and in the cerebral GM. Further confirmation of these results is warranted.

Supplementary Material

Refer to Web version on PubMed Central for supplementary material.

Acknowledgments

Funding statement

Research reported in this publication was funded by the National Center for Advancing Translational Sciences of the National Institutes of Health (NIH) under award Number UL1TR001412. The content is solely the responsibility of the authors and does not necessarily represent the official views of the NIH.

This study was funded in part by the The Annette Funicello Research Fund for Neurological Diseases and internal resources of the Buffalo Neuroimaging Analysis Center. In addition, we received support from the Jacquemin Family Foundation.

MS Journal Appendix for MRI methodology

Hardware	
Field strength	3T
Manufacturer	General Electric
Model	Signa Excite
Coil type (e.g. head, surface)	Multi-channel Head and Neck Coil
Number of coil channels	8

Acquisition sequence	
Type (e.g. FLAIR, DIR, DTI, fMRI)	FLAIR
Acquisition time	5:16
Orientation	Axial-oblique
Alignment (e.g. anterior commissure/poster commissure line)	parallel to the sub-callosal line
Voxel size	1×1×3

TR	8500ms	
TE	120ms	
TI	2100ms	
Flip angle	90	
NEX	1	
Field of view	25.6cm × 19.2cm	
Matrix size	256 × 192	
Parallel imaging	Yes	**No**
Acquisition sequence		
If used, parallel imaging method: (e.g. SENSE, GRAPPA)		
Cardiac gating	Yes	**No**
If used, cardiac gating method: (e.g. PPU or ECG)		
Contrast enhancement	Yes	**No**
If used, provide name of contrast agent, dose and timing of scan post-contrast administration		
Acquisition sequence		
Type (e.g. FLAIR, DIR, DTI, fMRI)	3D GRE	
Acquisition time	6:52	
Orientation	oblique	
Alignment (e.g. anterior commissure/poster commissure line)	parallel to the sub-callosal line	
Voxel size	1×1×3	
TR	50ms	
TE	6ms	
TI	/	
Flip angle	10	
NEX	1	
Field of view		
Matrix size	256 × 192	
Parallel imaging	Yes	**No**
Acquisition sequence		
If used, parallel imaging method: (e.g. SENSE, GRAPPA)		
Cardiac gating	Yes	**No**
If used, cardiac gating method: (e.g. PPU or ECG)		
Contrast enhancement	Yes	**No**
If used, provide name of contrast agent, dose and timing of scan post-contrast administration		
Acquisition sequence		
Type	3D T1-WI (IR-FSPGR)	

(e.g. FLAIR, DIR, DTI, fMRI)		
Acquisition time	9:18	
Orientation	Oblique	
Alignment (e.g. anterior commissure/poster commissure line)	anterior commissure/poster commissure line	
Voxel size	1×1×3	
TR	6.6ms	
TE	2.8ms	
TI	900ms	
Flip angle	10	
NEX	1	
Field of view	25.6cm × 19.2cm	
Matrix size	256 × 256	
Parallel imaging	Yes	**No**
If used, parallel imaging method: (e.g. SENSE, GRAPPA)		
Cardiac gating	Yes	**No**
If used, cardiac gating method: (e.g. PPU or ECG)		
Contrast enhancement	Yes	**No**
If used, provide name of contrast agent, dose and timing of scan post-contrast administration		
Acquisition sequence		
Other parameters:		

Hardware	
Field strength	1.5T
Manufacturer	General Electric
Model	Signa Excite
Coil type (e.g. head, surface)	Multi-channel Head and Neck Coil
Number of coil channels	8

Acquisition sequence	
Type (e.g. FLAIR, DIR, DTI, fMRI)	FLAIR
Acquisition time	3:12
Orientation	Axial-oblique
Alignment (e.g. anterior commissure/poster commissure line)	parallel to the sub-callosal line
Voxel size	1×1×3

TR	8000ms	
TE	126ms	
TI	2000ms	
Flip angle	90	
NEX	1	
Field of view	25.6cm × 19.2cm	
Matrix size	256 × 192	
Parallel imaging	Yes	**No**
Acquisition sequence		
If used, parallel imaging method: (e.g. SENSE, GRAPPA)		
Cardiac gating	Yes	**No**
If used, cardiac gating method: (e.g. PPU or ECG)		
Contrast enhancement	Yes	**No**
If used, provide name of contrast agent, dose and timing of scan post-contrast administration		
Acquisition sequence		
Type (e.g. FLAIR, DIR, DTI, fMRI)	3D T1-WI (IR-FSPGR)	
Acquisition time	8:50	
Orientation	Axial-oblique	
Alignment (e.g. anterior commissure/poster commissure line)	anterior commissure/poster commissure line	
Voxel size	1×1×3	
TR	5.9ms	
TE	3.7ms	
TI	9000ms	
Flip angle	10	
NEX	1	
Field of view	25.6cm × 19.2cm	
Matrix size	256 × 192	
Parallel imaging	Yes	**No**
If used, parallel imaging method: (e.g. SENSE, GRAPPA)		
Cardiac gating	Yes	**No**
If used, cardiac gating method: (e.g. PPU or ECG)		
Contrast enhancement	Yes	**No**
If used, provide name of contrast agent, dose and timing of scan post-contrast administration		
Acquisition sequence		
Type (e.g. FLAIR, DIR, DTI, fMRI)	3D GRE	

Acquisition time	5:00	
Orientation	Axial-oblique	
Alignment (e.g. anterior commissure/poster commissure line)	parallel to the sub-callosal line	
Voxel size	1×1×3	
TR	50ms	
TE	6ms	
TI	/	
Flip angle	10	
NEX	1	
Field of view	25.6cm × 19.2cm	
Matrix size	256 × 192	
Parallel imaging	Yes	**No**
If used, parallel imaging method: (e.g. SENSE, GRAPPA)		
Cardiac gating	Yes	**No**
If used, cardiac gating method: (e.g. PPU or ECG)		
Contrast enhancement	Yes	**No**
If used, provide name of contrast agent, dose and timing of scan post-contrast administration		

Image analysis methods and outputs	
Lesions	
Type (e.g. Gd-enhancing, T2-hyperintense, T1-hypointense)	T2 hyperintense lesions
Analysis method	Semi-automated edge detection contouring/ thresholding technique
Analysis software	JIM version 6.0
Output measure (e.g. count or volume [ml])	mL
Tissue measures (e.g. MTR, DTI, T1-RT, T2-RT, T2*, T2', ^{1}H-MRS, perfusion, Na)	
Type (e.g. whole brain, grey matter, white matter, spinal cord, normal-appearing grey matter or white matter)	Normal-appearing brain tissue, normal-appearing white matter, normal-appearing gray matter
Analysis method	SIENAX
Analysis software	FSL
Output measure	mL
Tissue measures (e.g. MTR, DTI, T1-RT, T2-RT, T2*, T2', ^{1}H-MRS, perfusion, Na)	
Type (e.g. whole brain, grey matter, white matter, spinal cord, normal-appearing grey matter or white matter)	MTR of normal-appearing brain tissue, normal-appearing white matter, normal-appearing gray matter
Analysis method	Subtraction of images with and without MT pulse
Analysis software	In house

Image analysis methods and outputs	
Output measure	Mean MTR value

References

1. Benedict RH and Zivadinov R. Risk factors for and management of cognitive dysfunction in multiple sclerosis. Nat Rev Neurol. 2011; 7: 332–42. [PubMed: 21556031]
2. Guan Y, Jakimovski D, Ramanathan M, Weinstock-Gutman B and Zivadinov R. The role of Epstein-Barr virus in multiple sclerosis: from molecular pathophysiology to in vivo imaging. Neural Regen Res. 2018.
3. Li R, Patterson KR and Bar-Or A. Reassessing B cell contributions in multiple sclerosis. Nat Immunol. 2018.
4. Jakimovski D, Weinstock-Guttman B, Ramanathan M, et al. Ocrelizumab: A B-cell Depleting Therapy for Multiple Sclerosis. Expert Opin Biol Ther. 2017.
5. Baker D, Marta M, Pryce G, Giovannoni G and Schmierer K. Memory B Cells are Major Targets for Effective Immunotherapy in Relapsing Multiple Sclerosis. EBioMedicine. 2017.
6. Morandi E, Jagessar SA, t Hart BA and Gran B. EBV Infection Empowers Human B Cells for Autoimmunity: Role of Autophagy and Relevance to Multiple Sclerosis. J Immunol. 2017.
7. Zivadinov R, Cerza N, Hagemeier J, et al. Humoral response to EBV is associated with cortical atrophy and lesion burden in patients with MS. Neurol Neuroimmunol Neuroinflamm. 2016; 3: e190. [PubMed: 26770996]
8. Horakova D, Zivadinov R, Weinstock-Guttman B, et al. Environmental factors associated with disease progression after the first demyelinating event: results from the multi-center SET study. PLoS One. 2013; 8: e53996. [PubMed: 23320113]
9. Poloni G, Minagar A, Haacke EM and Zivadinov R. Recent developments in imaging of multiple sclerosis. Neurologist. 2011; 17: 185–204. [PubMed: 21712664]
10. Schmierer K, Scaravilli F, Altmann DR, Barker GJ and Miller DH. Magnetization transfer ratio and myelin in postmortem multiple sclerosis brain. Ann Neurol. 2004; 56: 407–15. [PubMed: 15349868]
11. Chen JT, Easley K, Schneider C, et al. Clinically feasible MTR is sensitive to cortical demyelination in MS. Neurology. 2013; 80: 246–52. [PubMed: 23269598]
12. Dwyer M, Bergsland N, Hussein S, Durfee J, Wack D and Zivadinov R. A sensitive, noise-resistant method for identifying focal demyelination and remyelination in patients with multiple sclerosis via voxel-wise changes in magnetization transfer ratio. J Neurol Sci. 2009; 282: 86–95. [PubMed: 19386319]
13. Polman CH, Reingold SC, Banwell B, et al. Diagnostic criteria for multiple sclerosis: 2010 revisions to the McDonald criteria. Ann Neurol. 2011; 69: 292–302. [PubMed: 21387374]
14. Kurtzke JF. Rating neurologic impairment in multiple sclerosis: an expanded disability status scale (EDSS). Neurology. 1983; 33: 1444–52. [PubMed: 6685237]
15. Zivadinov R, Heininen-Brown M, Schirda CV, et al. Abnormal subcortical deep-gray matter susceptibility-weighted imaging filtered phase measurements in patients with multiple sclerosis: a case-control study. Neuroimage. 2012; 59: 331–9. [PubMed: 21820063]
16. Smith SM, Zhang Y, Jenkinson M, et al. Accurate, robust, and automated longitudinal and cross-sectional brain change analysis. Neuroimage. 2002; 17: 479–89. [PubMed: 12482100]
17. Gelineau-Morel R, Tomassini V, Jenkinson M, Johansen-Berg H, Matthews PM and Palace J. The effect of hypointense white matter lesions on automated gray matter segmentation in multiple sclerosis. Hum Brain Mapp. 2012; 33: 2802–14. [PubMed: 21976406]
18. Kvistad S, Myhr KM, Holmoy T, et al. Antibodies to Epstein-Barr virus and MRI disease activity in multiple sclerosis. Mult Scler. 2014; 20: 1833–40. [PubMed: 24842958]

19. Munger KL, Levin LI, O'Reilly EJ, Falk KI and Ascherio A. Anti-Epstein-Barr virus antibodies as serological markers of multiple sclerosis: a prospective study among United States military personnel. Mult Scler. 2011; 17: 1185–93. [PubMed: 21685232]
20. Nielsen TR, Rostgaard K, Nielsen NM, et al. Multiple sclerosis after infectious mononucleosis. Arch Neurol. 2007; 64: 72–5. [PubMed: 17210811]
21. Thacker EL, Mirzaei F and Ascherio A. Infectious mononucleosis and risk for multiple sclerosis: a meta-analysis. Ann Neurol. 2006; 59: 499–503. [PubMed: 16502434]
22. van der Mei I, Lucas RM, Taylor BV, et al. Population attributable fractions and joint effects of key risk factors for multiple sclerosis. Mult Scler. 2016; 22: 461–9. [PubMed: 26199349]
23. Farrell RA, Antony D, Wall GR, et al. Humoral immune response to EBV in multiple sclerosis is associated with disease activity on MRI. Neurology. 2009; 73: 32–8. [PubMed: 19458321]
24. Zivadinov R, Zorzon M, Weinstock-Guttman B, et al. Epstein-Barr virus is associated with grey matter atrophy in multiple sclerosis. J Neurol Neurosurg Psychiatry. 2009; 80: 620–5. [PubMed: 19168469]
25. Virtanen JO, Wohler J, Fenton K, Reich DS and Jacobson S. Oligoclonal bands in multiple sclerosis reactive against two herpesviruses and association with magnetic resonance imaging findings. Mult Scler. 2014; 20: 27–34. [PubMed: 23722324]
26. Moreno MA, Or-Geva N, Aftab BT, et al. Molecular signature of Epstein-Barr virus infection in MS brain lesions. Neurol Neuroimmunol Neuroinflamm. 2018; 5: e466. [PubMed: 29892607]
27. Veroni C, Serafini B, Rosicarelli B, Fagnani C and Aloisi F. Transcriptional profile and Epstein-Barr virus infection status of laser-cut immune infiltrates from the brain of patients with progressive multiple sclerosis. J Neuroinflammation. 2018; 15: 18. [PubMed: 29338732]
28. Serafini B, Scorsi E, Rosicarelli B, Rigau V, Thouvenot E and Aloisi F. Massive intracerebral Epstein-Barr virus reactivation in lethal multiple sclerosis relapse after natalizumab withdrawal. J Neuroimmunol. 2017; 307: 14–7. [PubMed: 28495131]
29. Magliozzi R, Serafini B, Rosicarelli B, et al. B-cell enrichment and Epstein-Barr virus infection in inflammatory cortical lesions in secondary progressive multiple sclerosis. J Neuropathol Exp Neurol. 2013; 72: 29–41. [PubMed: 23242282]
30. Serafini B, Rosicarelli B, Magliozzi R, Stigliano E and Aloisi F. Detection of ectopic B-cell follicles with germinal centers in the meninges of patients with secondary progressive multiple sclerosis. Brain Pathol. 2004; 14: 164–74. [PubMed: 15193029]
31. Serafini B, Rosicarelli B, Franciotta D, et al. Dysregulated Epstein-Barr virus infection in the multiple sclerosis brain. J Exp Med. 2007; 204: 2899–912. [PubMed: 17984305]
32. Howell OW, Reeves CA, Nicholas R, et al. Meningeal inflammation is widespread and linked to cortical pathology in multiple sclerosis. Brain. 2011; 134: 2755–71. [PubMed: 21840891]
33. Magliozzi R, Howell OW, Reeves C, et al. A Gradient of neuronal loss and meningeal inflammation in multiple sclerosis. Ann Neurol. 2010; 68: 477–93. [PubMed: 20976767]
34. Zurawski J, Lassmann H and Bakshi R. Use of Magnetic Resonance Imaging to Visualize Leptomeningeal Inflammation in Patients With Multiple Sclerosis: A Review. JAMA Neurol. 2017; 74: 100–9. [PubMed: 27893883]
35. Absinta M, Vuolo L, Rao A, et al. Gadolinium-based MRI characterization of leptomeningeal inflammation in multiple sclerosis. Neurology. 2015; 85: 18–28. [PubMed: 25888557]
36. Bevan RJ, Evans R, Griffiths L, et al. Meningeal Inflammation and Cortical Demyelination in Acute Multiple Sclerosis. Ann Neurol. 2018.
37. Lehmann-Horn K, Kinzel S, Feldmann L, et al. Intrathecal anti-CD20 efficiently depletes meningeal B cells in CNS autoimmunity. Ann Clin Transl Neurol. 2014; 1: 490–6. [PubMed: 25356419]
38. Bhargava P, Wicken C, Smith M, et al. Phase 1 Trial of Intrathecal Rituximab in Progressive MS Patients with Evidence of Leptomeningeal Contrast Enhancement (P3.393). Neurology. 2018; 90: P3.393.
39. Trapp BD, Vignos M, Dudman J, et al. Cortical neuronal densities and cerebral white matter demyelination in multiple sclerosis: a retrospective study. Lancet Neurol. 2018.
40. Absinta M, Sati P, Fechner A, Schindler MK, Nair G and Reich DS. Identification of Chronic Active Multiple Sclerosis Lesions on 3T MRI. AJNR Am J Neuroradiol. 2018.

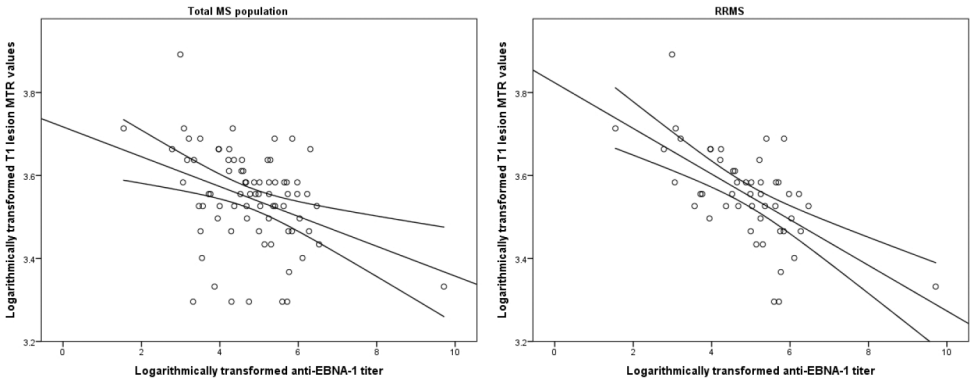

Figure 1.

Scatter-plot representation of the associations between anti-EBNA-1 titer levels and magnetization transfer ratio values of T1-hypointense lesions in all multiple sclerosis patients (left) and relapsing-remitting multiple sclerosis patients only (right)

MTR – magnetization transfer ratio, EBNA-1 – Epstein-Barr nuclear antigen-1. Due to the non-normal distribution of data, the anti-EBNA-1 titer was transformed using the natural logarithm and Pearson's correlation is fitted.

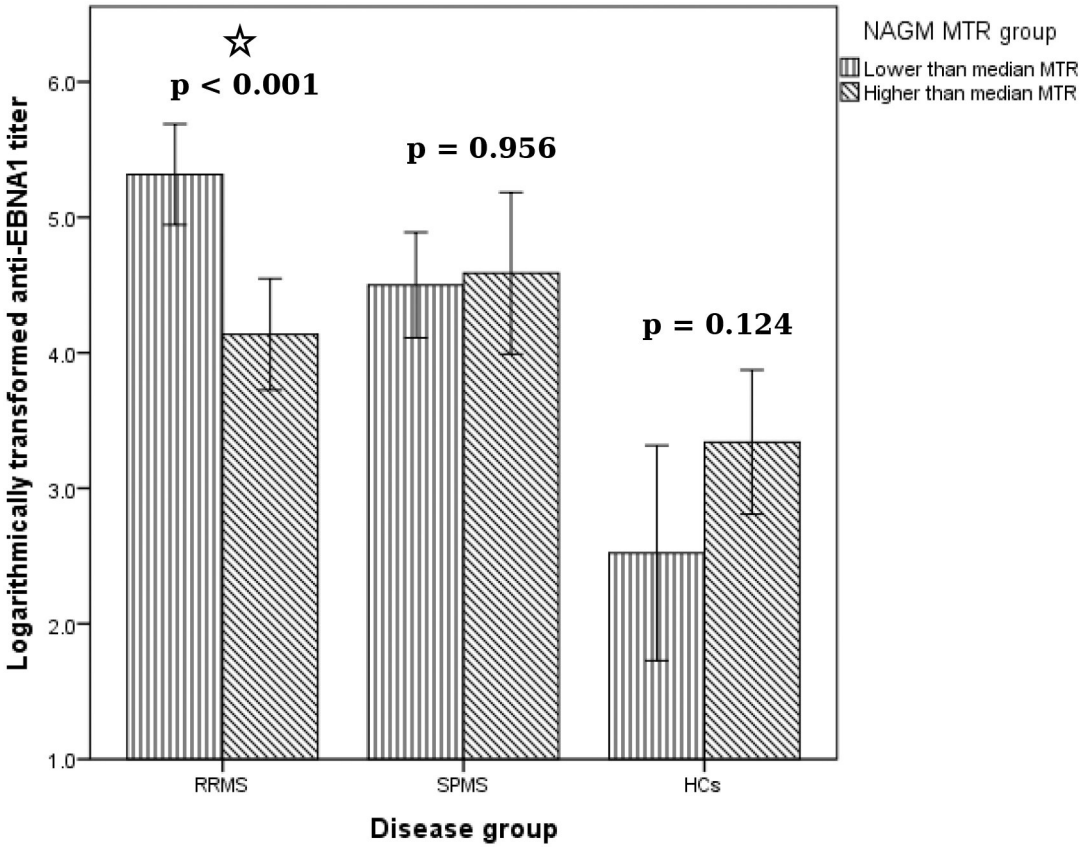

Figure 2.

Dichotomous comparison of anti-EBNA-1 titer between lower and higher NAGM MTR median values in MS subpopulations and in healthy controls.

EBNA-1 – Epstein-Barr nuclear antigen-1, NAGM – normal appearing gray matter, MTR – magnetization transfer ratio, RRMS – relapsing remitting multiple sclerosis, SPMS – secondary progressive multiple sclerosis, HCs – healthy controls.

P-values were derived with Mann-Whitney U test. Error bars demonstrate 95% confidence interval.

A significant difference (*) in anti-EBNA1 titer between RRMS with lower vs. higher half of MTR values.

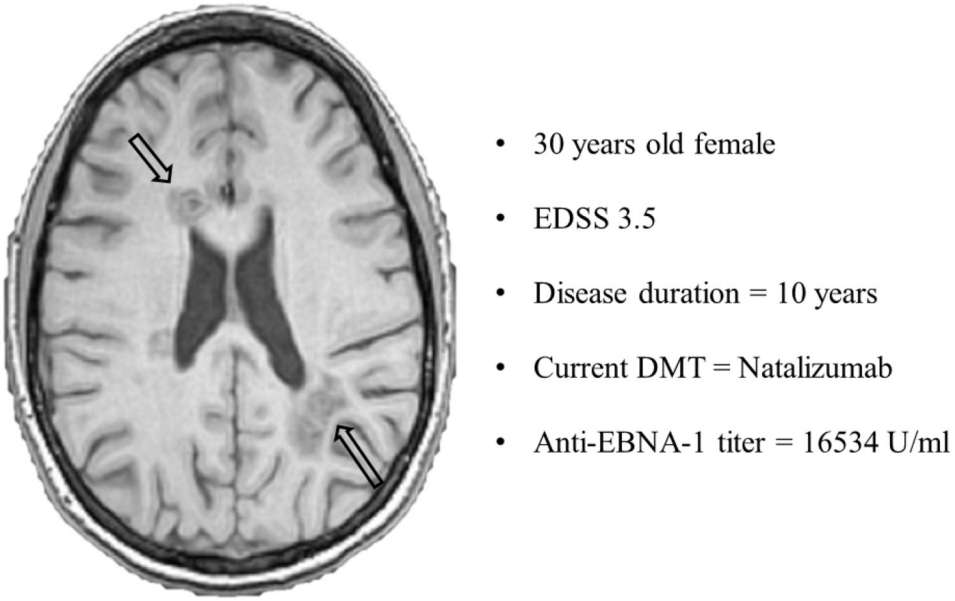

Figure 3.

Example of relapsing-remitting multiple sclerosis patients with very high anti-EBNA-1 titer and presence of T1-hypointensities

The patient had relatively low disease duration of 10 years, EDSS score of 3.5 and was on natalizumab treatment. At the time of serum sample examination, the patient presented with abnormally high titer of anti-EBNA-1 antibodies. The corresponding lesioned MRI features include 11 T1-hypointense lesions with total volume of 12.2ml and 12 T2-hyperintense lesions with total volume of 22.4ml. EDSS – Expanded Disability Status Scale, DMT – disease modifying therapy, EBNA-1 – Epstein Barr nuclear antigen-1.

Table 1.

Demographic, clinical, and magnetization transfer ratio characteristics of the multiple sclerosis patients and the healthy controls.

	HCs (n=41)	MS (n=101)	p-value	BH-adjusted p-value
Female, n (%)	29 (70.7%)	75 (74.3%)	0.679	0.679
Age, mean (SD)	45.4 (12.6)	46.9 (10.3)	0.469	0.681
Disease duration, mean (SD)	-	13.3 (10.9)	-	-
RRMS/SPMS	-	69/32	-	-
EDSS, median (IQR)	-	2.5 (1.5–5.0)	-	-
History of infectious mononucleosis, n (%)	7 (17.1%)	34 (33.7%)	0.067	0.126
Anti-EBNA-1 titer, median (IQR)	27.8 (8.9–48.7)	107.9 (47.1–245.9)	**<0.001**	**<0.001**
Disease-modifying treatment				
Interferon-β	-	37 (36.6)	-	-
Glatiramer acetate	-	25 (24.8)	-	-
Natalizumab	-	20 (19.8)	-	-
Off-label medications	-	4 (3.9)	-	-
No DMT use	-	15 (14.9)	-	-
MTR outcomes measures				
T2 lesion MTR	45.0 (43.0–47.0)	41.0 (36.0–44.0)	**<0.001**	**<0.001**
T1 lesion MTR	-	35.0 (32.3–38.0)	-	-
NABT MTR	42.0 (42.0–45.0)	40.0 (37.0–42.0)	**<0.001**	**<0.001**
NAWM MTR	46.0 (45.0–49.0)	44.0 (39.0–45.0)	**<0.001**	**<0.001**
NAGM MTR	39.0 (38.0–42.0)	37.0 (34.5–38.0)	**<0.001**	**<0.001**

HC – healthy controls, MS – multiple sclerosis, BH – Benjamini-Hochberg, RRMS – relapsing-remitting multiple sclerosis, SPMS – secondary-progressive multiple sclerosis, EDSS – Extended Disability Status Scale, EBV – Epstein-Barr virus, EBNA-1 – Epstein-Barr nuclear antigen-1, MTR – magnetization transfer ratio, , NABT – normal appearing brain tissue, NAWM – normal appearing white matter, NAGM – normal appearing gray matter.

The MTR and EBV response measures are shown as median (IQR). χ^2, Student's t-test, and Mann Whitney U-test were used accordingly. Benjamini-Hochberg-adjusted p values < 0.05 were considered significant.

Off-label medications include mycophenolic acid (2), intravenous immunoglobulins (1) and naltrexone (1). The patient treated with intravenous immunoglobulins (IVIG) received the IVIG infusions after a relapse which occurred 10 months before study entry.

MTR value comparison utilizing only 3T-scanned MS patients and 3T HCs yielded similar statistical differences (T2 p=0.005, NAWM p=0.001, NAGM p<0.001, and NABT p<0.001).

Table 2.

Demographic, clinical, and magnetization transfer ratio characteristics of the relapsing remitting and progressive multiple sclerosis patients.

	RRMS (n=69)	SPMS (n=32)	p-value	BH-adjusted p-value
Female, n (%)	51 (73.9%)	24 (75.0%)	1.000	1.000
Age, mean (SD)	44.4 (10.0)	52.3 (8.7)	**<0.001**	**0.001**
Disease duration, mean (SD)	10.2 (8.4)	19.9 (12.8)	**<0.001**	**0.002**
EDSS, median (IQR)	2.0 (1.5–2.5)	6.0 (4.5–6.5)	**<0.001**	**<0.001**
Anti-EBNA-1 titer	132.6 (49.5–279.9)	80.4 (41.2–217.0)	0.317	0.635
	MTR outcomes measures			
T2 lesion MTR	41.0 (36.0–44.0)	42.0 (35.0–43.0)	0.909	0.957
T1 lesion MTR	35.0 (33.0–37.5)	35.0 (32.0–38.0)	0.694	0.992
NABT MTR	41.0 (36.5–42.0)	40.0 (37.0–41.0)	0.476	0.865
NAWM MTR	44.0 (38.0–46.0)	44.0 (39.3–45.0)	0.727	0.808
NAGM MTR	37.0 (34.0–38.5)	36.5 (34.3–38.0)	0.269	0.599

RRMS – relapsing-remitting multiple sclerosis, SPMS – secondary-progressive multiple sclerosis, BH – Benjamini-Hochberg, EDSS – Extended Disability Status Scale, EBV – Epstein-Barr virus, EBNA-1 – Epstein-Barr nuclear antigen-1, MTR – magnetization transfer ratio, NABT – normal appearing brain tissue, NAWM – normal appearing white matter, NAGM – normal appearing gray matter.

The MTR and EBV response measures are shown as median (IQR). χ^2, Student's t-test, and Mann Whitney U-test were used accordingly. Benjamini-Hochberg-adjusted p values < 0.05 were considered significant.

Comparison of patients scanned only on 3T scanner yielded similar statistical differences.

Table 3.

Associations between the level of humoral Epstein-Barr virus response (anti-EBNA-1 titer) and magnetization transfer ratio outcome measures in multiple sclerosis and healthy controls.

	HCs (n=41)			MS (n=101)		
	r_s-value	p-value	BH-adjusted p-value	r_s-value	p-value	BH-adjusted p-value
T2 lesion MTR	0.087	0.641	0.681	**−0.210**	**0.041**	0.087
T1 lesion MTR	-	-	-	**−0.287**	**0.012**	**0.035**
NABT MTR	0.206	0.195	0.237	−0.168	0.095	0.161
NAWM MTR	0.235	0.139	0.186	−0.152	0.132	0.186
NAGM MTR	0.246	0.121	0.186	**−0.215**	**0.032**	0.077

HC – healthy controls, MS – multiple sclerosis, BH – Benjamini-Hochberg, MTR – magnetization transfer ratio, NABT – normal appearing brain tissue, NAWM – normal appearing white matter, NAGM – normal appearing gray matter.

Spearman's ranked correlations (for the HCs) and partial non-parametric correlations adjusted for scanner field strength (for MS) were used. Benjamini-Hochberg-adjusted p values < 0.05 were considered significant.

Table 4.

Associations between the level of humoral Epstein-Barr virus response (anti-EBNA-1 titer) and magnetization transfer ratio outcome measures in relapsing-remitting and progressive multiple sclerosis patients.

	RRMS (n=69)			SPMS (n=32)		
	r_s-value	p-value	BH-adjusted p-value	r_s-value	p-value	BH-adjusted p-value
T2 lesion MTR	**−0.261**	**0.037**	0.124	−0.132	0.487	0.812
T1 lesion MTR	**−0.524**	**<0.001**	**0.001**	−0.075	0.716	0.895
NABT MTR	−0.227	0.062	0.178	−0.066	0.723	0.851
NAWM MTR	−0.164	0.180	0.451	−0.112	0.550	0.847
NAGM MTR	**−0.308**	**0.011**	**0.043**	−0.068	0.715	0.953

RRMS – relapsing-remitting multiple sclerosis, SPMS – secondary-progressive multiple sclerosis, MTR – magnetization transfer ratio, NABT – normal appearing brain tissue, NAWM – normal appearing white matter, NAGM – normal appearing gray matter.

Partial non-parametric correlation adjusted for scanner field strength were used. Benjamini-Hochberg-adjusted p values <0.05 were considered significant.